

# Relativistic calculations of the $U^{91+}(1s)-U^{92+}$ collision using the finite basis set of cubic Hermite splines on a lattice in coordinate space

G. B. Deyneka,<sup>1</sup> I. A. Maltsev,<sup>2</sup> I. I. Tupitsyn,<sup>2</sup> V. M. Shabaev,<sup>2</sup>  
A. I. Bondarev,<sup>2</sup> Y. S. Kozhedub,<sup>2</sup> G. Plunien,<sup>3</sup> and Th. Stöhlker<sup>4,5,6</sup>

<sup>1</sup> *St. Petersburg State University of Information Technologies,  
Mechanics and Optics, Kronverk av. 49, 197101 St. Petersburg, Russia*

<sup>2</sup> *Department of Physics, St. Petersburg State University,  
Uljanovskaya 1, Petrodvorets, 198504 St. Petersburg, Russia*

<sup>3</sup> *Institut für Theoretische Physik, Technische Universität Dresden,  
Mommensenstraße 13, D-01062 Dresden, Germany*

<sup>4</sup> *GSI Helmholtzzentrum für Schwerionenforschung GmbH,  
Planckstrasse 1, D-64291 Darmstadt, Germany*

<sup>5</sup> *Helmholtz-Institute Jena, D-07743 Jena, Germany*

<sup>6</sup> *Institut für Optik und Quantenelektronik,  
Friedrich-Schiller-Universität, D-07743 Jena, Germany*

## Abstract

A new method for solving the time-dependent two-center Dirac equation is developed. The approach is based on the using of the finite basis of cubic Hermite splines on a three-dimensional lattice in the coordinate space. The relativistic calculations of the excitation and charge-transfer probabilities in the low-energy  $U^{91+}(1s)-U^{92+}$  collisions in two and three dimensional approaches are performed. The obtained results are compared with our previous calculations employing the Dirac-Sturm basis sets [I. I. Tupitsyn *et al.*, Phys. Rev. A **82**, 042701 (2010)]. The role of the negative-energy Dirac spectrum is investigated within the monopole approximation.

PACS numbers: 34.10.+x, 34.50.-s, 34.70.+e

## I. INTRODUCTION

Heavy-ion collisions play a very important role in studying relativistic quantum dynamics of electrons in the presence of strong electromagnetic fields [1–4]. Such collisions can also give a unique tool for tests of quantum electrodynamics at the supercritical fields, provided the projectile energy approaches the Coulomb barrier (about 6 MeV/u for the U-U collisions) [5]. To date various theoretical methods were developed for calculations of heavy-ion collisions. Among them are the lattice methods for solving the time-dependent Dirac equation in the coordinate space [6–12] and in the momentum space [13, 14].

In the case of head-on collisions, due to the rotational symmetry with respect to the internuclear axis, the three-dimensional (3D) process is easily reduced to the two-dimensional (2D) one. Moreover, to simplify the numerical procedure, the 2D approximation can be applied for the 3D collision with nonzero impact parameter as well. This simplification was used in Refs. [6, 8], where the calculations were performed by the finite difference method on a two-dimensional grid.

In Refs. [15–18] the basis sets of atomic eigenstates were employed to study heavy-ion collisions at high energies. The authors of Refs. [19, 20] studied various processes in low-energy ion-atom collisions with the use of relativistic molecular orbitals. In works [21–24] some effects were investigated in so-called monopole approximation, which allows one to reduce the 2D and 3D two-center Dirac equations to the spherically symmetric one-center radial equation. The monopole approximation was found to be very useful for studying processes at short internuclear distances [25]. Unfortunately, this approach as well as its one-center extensions beyond the monopole approximation [26, 27] can not be applied to calculations of charge-transfer processes.

Recently [28–30] we developed a method which allows solving the time-dependent two-center Dirac equation in the basis of atomic-like Dirac-Fock-Sturm orbitals. With this method we could calculate the electron-excitation and charge-transfer probabilities in low-energy ion-ion and ion-atom collisions.

Despite the diversity of the methods developed, none of them provide the full relativistic treatment of the quantum dynamics of electrons in low-energy heavy-ion collisions beyond the monopole approximation. In particular, it means that with these methods we can not calculate the charge-transfer probability for the low-energy collision with the proper account for the dynamics of the occupied negative-energy states. This problem, which seems especially important for studying the supercritical regime, remains unsolved even for the simplest one-electron case. Moreover, the rather successful application of the method of Ref. [28] for calculations of the charge-transfer and total ionization probabilities

and its generalization to study the excitation and charge transfer with many-electron systems [29, 30] does not guarantee that the finite basis set representation based on the atomic-like orbitals can properly describe the two-center continuum states.

In the present paper, which should be considered as a continuation of our previous investigations [28–32], we work out an alternative approach to calculations of electron-excitation and charge-transfer probabilities in low-energy heavy-ion collisions. In this method, the time-dependent Dirac wave function is expanded in the basis of Hermite cubic splines at a fixed grid. Such a basis was previously successfully used in the 1D and 2D time-dependent nonrelativistic calculations [33, 34].

The Hermite splines are a special choice of well-known  $B$ -splines [35]. During the last decades the  $B$ -splines were successfully applied for solving the one-center Dirac equation [36, 37] as well as the two-center nonrelativistic Schrödinger [38] and relativistic Dirac [27, 39] problems. The Hermite splines have been used to obtain accurate solutions of the nonrelativistic Hartree-Fock [40, 41] and relativistic Dirac-Fock equations [42] for diatomic molecules. An accurate finite element method using cubic Hermite splines was also recently developed for atomic calculations within the density functional theory and the Hartree-Fock method [43]. The convergence with respect to the total number of the basis functions was investigated for Hermite splines of different order and it was concluded that the cubic splines provide an optimum choice with respect to the convergence and the simplicity of analytic expressions derived for the matrix elements [43]. The basis of the cubic Hermite splines is shortly discussed in Sec. II B of the present paper.

In Sec. II we describe the procedure of solving the one-electron time-dependent Dirac equation in the finite basis of the Hermite cubic splines. The monopole (1D), axially symmetric (2D) and full 3D approaches are formulated. Basic formulas for the transition amplitudes, including those which properly account for the negative-energy spectrum contribution, are also given. In Sec. III the results of our calculations of the excitation and charge-transfer probabilities for the  $\text{U}^{91+}(1s)\text{--}\text{U}^{92+}$  collision at the projectile energy  $E = 6 \text{ MeV/u}$  are presented and compared with the previous calculations.

Atomic units ( $\hbar = e = m = 1$ ) are used throughout the paper.

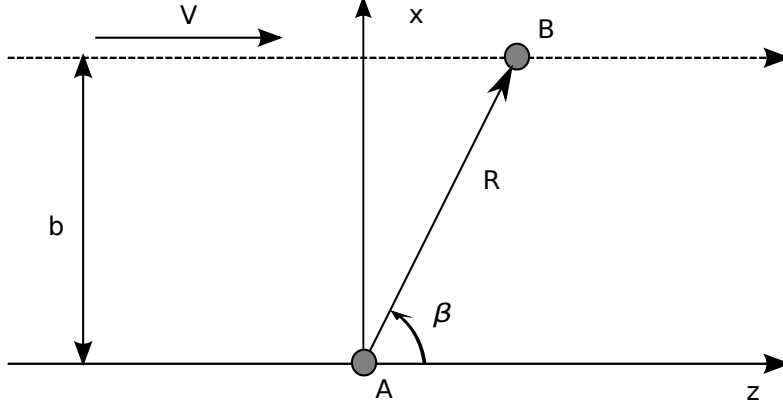


FIG. 1: The straight-line trajectory of the ion-ion collision. The target  $A$  is stationary, while the projectile  $B$  moves along a straight line with the velocity  $v$ .  $R$  is the distance between the target  $A$  and the projectile  $B$ , and  $b$  is the impact parameter.

## II. METHODS OF CALCULATION

### A. Time-dependent Dirac equation in a finite basis

In our consideration we employ the semiclassical approximation, where the atomic nuclei are treated as sources of a time-dependent external potential. What is more, instead of using the classical (Rutherford) trajectories, in our calculations we assume that the projectile ( $\text{U}^{92+}$ ) moves along a straight line with a constant velocity, while the position of the target ( $\text{U}^{91+}(1s)$ ) is fixed (Fig. 1). The electron motion is described by the time-dependent Dirac equation

$$i \frac{\partial}{\partial t} \psi(\mathbf{r}, t) = \hat{H} \psi(\mathbf{r}, t), \quad \hat{H} = c \boldsymbol{\alpha} \cdot \mathbf{p} + (\beta - 1)c^2 + V(\mathbf{r}, t), \quad (1)$$

where  $\psi(\mathbf{r}, t)$  denotes the Dirac bispinor and  $\boldsymbol{\alpha}$ ,  $\beta$  are the Dirac matrices. The two-center potential  $V(\mathbf{r}, t)$  consists of the nuclear Coulomb potentials of the target and projectile

$$V(\mathbf{r}, t) = V_{\text{nucl}}^A(r_A) + V_{\text{nucl}}^B(r_B), \quad (2)$$

where indices  $A$  and  $B$  correspond to the target and projectile, respectively.

Eq. (1) is solved using the coupled-channel approach with time-independent finite basis set  $\{\varphi_k(\mathbf{r})\}$ :

$$\psi(\mathbf{r}, t) = \sum_k C_k(t) \varphi_k(\mathbf{r}), \quad (3)$$

$$i S \frac{d\mathbf{C}(t)}{dt} = H(t) \mathbf{C}(t). \quad (4)$$

Here  $\mathbf{C}$  is the vector which incorporates the expansion coefficients  $C_k(t)$ ,  $H$  and  $S$  are the Hamiltonian and overlapping matrices,

$$H_{kj} = \langle \varphi_k | \hat{H} | \varphi_j \rangle, \quad S_{kj} = \langle \varphi_k | \varphi_j \rangle. \quad (5)$$

We note that in contrast to our previous work [28], where the time-dependent basis functions were employed, the differential matrix equation (4) has a simpler form. To solve equation (4) we apply the Crank-Nicolson (CN) method [44, 45]. In this method a short-time evolution operator,  $\psi(t + \Delta t) = \hat{U}_{\text{CN}}(t + \Delta t, t)\psi(t)$ , is approximated by

$$\hat{U}_{\text{CN}}(t + \Delta t, t) = \left[ 1 + \frac{i \Delta t}{2} \hat{H}(t + \Delta t/2) \right]^{-1} \left[ 1 - \frac{i \Delta t}{2} \hat{H}(t + \Delta t/2) \right]. \quad (6)$$

$\hat{U}_{\text{CN}}$ , being a unitary operator, conserves the norm of the wave function. The CN method is known as stable and accurate up to the  $(\Delta t)^2$  terms included.

With the CN method, the time-dependent equation (4) can be written as

$$\mathbf{C}(t + \Delta t) = U_{\text{CN}}(t + \Delta t, t) \mathbf{C}(t), \quad (7)$$

where

$$U_{\text{CN}}(t + \Delta t, t) = \left[ 1 + \frac{i \Delta t}{2} S^{-1} H(t + \Delta t/2) \right]^{-1} \left[ 1 - \frac{i \Delta t}{2} S^{-1} H(t + \Delta t/2) \right]. \quad (8)$$

We emphasize that, in contrast to the operator  $\hat{U}_{\text{CN}}$ , the matrix  $U_{\text{CN}}$  is not unitary, since the matrices  $S$  and  $H$  do not commute. However, the matrix  $U_{\text{CN}}$  also preserves the wave function norm (see the Appendix)

$$\langle \psi(t + \Delta t) | \psi(t + \Delta t) \rangle = \mathbf{C}^\dagger(t + \Delta t) S \mathbf{C}(t + \Delta t) = \langle \psi(t) | \psi(t) \rangle = 1. \quad (9)$$

To determine the coefficients  $\mathbf{C}(t + \Delta t)$  at each time step we have to solve the following system of linear equations

$$\left[ S + \frac{i \Delta t}{2} H \right] \mathbf{C}(t + \Delta t) = \left[ S - \frac{i \Delta t}{2} H \right] \mathbf{C}(t). \quad (10)$$

## B. Basis of cubic Hermite splines

In this paper we use a basis of piecewise Hermite cubic splines. Let us consider a partition of the interval  $[a, b]$  into  $N$  subintervals:  $a = x_0 < x_1 < \dots < x_N = b$ , with the length  $h_\alpha = x_\alpha - x_{\alpha-1}$

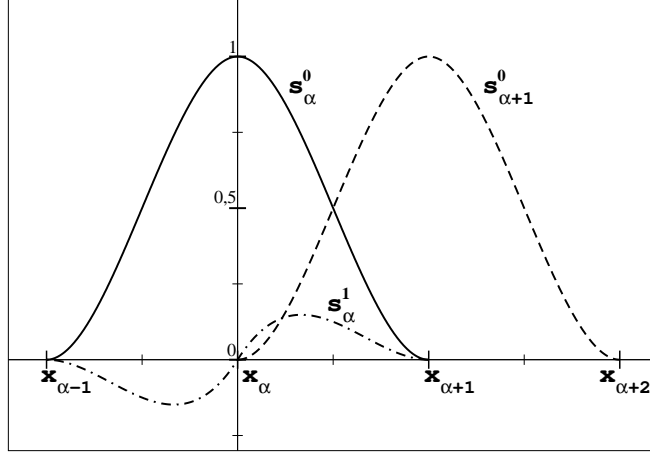


FIG. 2: The Hermite basis splines.

of the  $\alpha$ -th interval. We introduce two basis piecewise functions  $s_{\alpha}^0(x)$  and  $s_{\alpha}^1(x)$  for each point  $x_{\alpha}$  ( $\alpha = 1, \dots, N-1$ ) [35]:

$$s_{\alpha}^0(x) = \begin{cases} \frac{(x - x_{\alpha-1})^2}{h_{\alpha}^3} [2(x_{\alpha} - x) + h_{\alpha}] & x_{\alpha-1} \leq x \leq x_{\alpha} \\ \frac{(x_{\alpha+1} - x)^2}{h_{\alpha+1}^3} [2(x_{\alpha} - x) + h_{\alpha+1}] & x_{\alpha} \leq x \leq x_{\alpha+1} \\ 0 & \text{otherwise} \end{cases} \quad (11)$$

and

$$s_{\alpha}^1(x) = \begin{cases} \frac{(x - x_{\alpha-1})^2}{h_{\alpha}^2} (x - x_{\alpha}) & x_{\alpha-1} \leq x \leq x_{\alpha} \\ \frac{(x_{\alpha+1} - x)^2}{h_{\alpha+1}^2} (x - x_{\alpha}) & x_{\alpha} \leq x \leq x_{\alpha+1} \\ 0 & \text{otherwise} \end{cases} \quad (12)$$

The values of these functions and their first derivatives at the nodal points are given by

$$s_{\alpha}^0(x_{\beta}) = \delta_{\alpha,\beta}, \quad \frac{ds_{\alpha}^0}{dx}(x_{\beta}) = 0, \quad s_{\alpha}^1(x_{\beta}) = 0, \quad \frac{ds_{\alpha}^1}{dx}(x_{\beta}) = \delta_{\alpha,\beta}. \quad (13)$$

The functions  $s_{\alpha}^0$  and  $s_{\alpha}^1$  are displayed in Fig. 2. Both Hermite splines  $s_{\alpha}^{\mu}$  ( $\mu = 0, 1$ ) are continuously differentiable at all points, in contrast to the second derivatives, which are discontinuous at the points  $x_{\alpha-1}$ ,  $x_{\alpha}$ , and  $x_{\alpha+1}$ . Since the  $s_{\alpha}^{\mu}$  splines vanish outside the interval  $(x_{\alpha-1}, x_{\alpha+1})$ , we can write

$$s_{\alpha}^{\mu}(x) s_{\beta}^{\nu}(x) = 0 \quad \text{if} \quad |\alpha - \beta| \geq 2, \quad (\mu, \nu = 0, 1). \quad (14)$$

Therefore the Hamiltonian and overlapping matrices in this basis are sparse.

The Hermite cubic interpolation expansion for a function  $f(x)$  with the boundary conditions  $f(a) = f(b) = f'(a) = f'(b) = 0$  is given by a rather simple equation:

$$f(x) = \sum_{\alpha=1}^{N-1} [f(x_{\alpha}) s_{\alpha}^0(x) + f'(x_{\alpha}) s_{\alpha}^1(x)] . \quad (15)$$

It should be noted that the piecewise Hermite cubic spline interpolation is one of the best choice of the cubic spline interpolation schemes [35].

### C. Monopole approximation (1D)

In this subsection we consider the collision of a bare nucleus (projectile) with a H-like heavy ion (target) in the central-field (monopole) approximation. Within this approximation only the monopole part of the reexpansion of the projectile Coulomb potential at the target center is taken into account:

$$V_{\text{mon}}^B(r, t) = \begin{cases} -\frac{Z}{r} & r \geq R(t) \\ -\frac{Z}{R(t)} & r < R(t) \end{cases} . \quad (16)$$

Here  $R(t)$  denotes the time-dependent distance between the target  $A$  (at the rest) and the moving projectile  $B$ , and, for simplicity, the point-charge nuclear model is used.

We should stress that in our one-center monopole approximation the electron-nucleus interaction potential is centered at the target ( $A$ ) position, in contrast to the center of nuclear mass position, which was employed in Refs. [21–23].

In the central-field approximation the time-dependent wave function  $\psi(\mathbf{r}, t)$  is the Dirac bispinor

$$\psi_{n\kappa m}(\mathbf{r}, t) = \begin{pmatrix} \frac{P_{n\kappa}(r, t)}{r} \chi_{\kappa m}(\Omega) \\ i \frac{Q_{n\kappa}(r, t)}{r} \chi_{-\kappa m}(\Omega) \end{pmatrix} , \quad (17)$$

where  $P_{n\kappa}(r, t)$  and  $Q_{n\kappa}(r, t)$  are the large and small radial components, respectively,  $\chi_{\kappa m}(\Omega)$  is the spherical spinor, and  $\kappa = (-1)^{l+j+1/2}(j + 1/2)$  is the Dirac angular quantum number.

The time-dependent radial Dirac equation can be written in the form

$$\begin{cases} i \frac{\partial}{\partial t} P(r, t) = c \left[ -\frac{d}{dr} + \frac{\kappa}{r} \right] Q(r, t) + [V^A(r) + V_{\text{mon}}^B(r, t)] P(r, t) \\ i \frac{\partial}{\partial t} Q(r, t) = c \left[ \frac{d}{dr} + \frac{\kappa}{r} \right] P(r, t) + [V^A(r) + V_{\text{mon}}^B(r, t) - 2c^2] Q(r, t) \end{cases} , \quad (18)$$

where  $c$  is the speed of light. The functions  $P(r, t)$  and  $Q(r, t)$  are expanded in the finite basis set of cubic Hermite splines  $s_\alpha^\mu(r)$  with the Hermite components ( $\mu = 0, 1$ )

$$\begin{cases} P(r, t) = \sum_{\alpha, \mu} C_{\alpha\mu}^P(t) s_\alpha^\mu(r) \\ Q(r, t) = \sum_{\alpha, \mu} C_{\alpha\mu}^Q(t) s_\alpha^\mu(r) \end{cases}. \quad (19)$$

Substituting this expansion into Eq. (18) leads to the time-dependent matrix equation for the vector of coefficients  $\mathbf{C}(t)$ :

$$i \frac{\partial}{\partial t} \mathbf{C}(t) = S^{-1} H(t) \mathbf{C}(t), \quad \mathbf{C}(t) = \begin{pmatrix} \mathbf{C}^P(t) \\ \mathbf{C}^Q(t) \end{pmatrix}, \quad (20)$$

where  $S$  is the overlapping matrix and  $H(t)$  is the matrix of the radial Dirac operator  $\hat{H}(t)$ ,

$$\hat{H}(t) = \begin{pmatrix} V^A(r) + V_{\text{mon}}^B(r, t) & c \left[ -\frac{d}{dr} + \frac{\kappa}{r} \right] \\ c \left[ \frac{d}{dr} + \frac{\kappa}{r} \right] & V^A(r) + V_{\text{mon}}^B(r, t) - 2c^2 \end{pmatrix}. \quad (21)$$

Eq. (20) is solved by the CN method with  $\mathbf{C}(t = -\infty)$  corresponding to the  $1s$  state of the target H-like ion.

The monopole approximation is rather crude at large internuclear distances and can not be applied to investigation of the charge-transfer processes. However, the simple one-center calculations give some useful information about electron-excitation and ionization processes, and can be used to estimate the role of the negative-energy Dirac continuum.

#### D. Axially-symmetric field (2D)

In this subsection we describe the 2D approach for heavy-ion collisions. In this approach the process is approximated by the head-on collision and the time-dependence of the internuclear distance is assumed to be equal to  $R(t) = \sqrt{Z^2(t) + b^2}$  (see Fig. 1).

Since in the case under consideration the external field is axially symmetric, the Dirac operator  $\hat{H}$  commutes with the  $z$ -component  $\hat{J}_z$  of the total angular momentum of the electron. Then the wave function can be chosen as an eigenfunction of the operator  $\hat{J}_z$ ,

$$\hat{J}_z \psi_m(\mathbf{r}, t) = m \psi_m(\mathbf{r}, t) \quad (22)$$



with a half-integer quantum number  $m$ .

In the cylindrical coordinates  $(\rho, \phi, z)$  the 4-component wave function  $\psi_m(\mathbf{r}, t)$  can be written as

$$\psi_m(\rho, \phi, z, t) = \frac{1}{\sqrt{2\pi}} \frac{1}{\sqrt{\rho}} \begin{pmatrix} U_m^1(\rho, z, t) \exp[i(m - \frac{1}{2})\phi] \\ U_m^2(\rho, z, t) \exp[i(m + \frac{1}{2})\phi] \\ iU_m^3(\rho, z, t) \exp[i(m - \frac{1}{2})\phi] \\ iU_m^4(\rho, z, t) \exp[i(m + \frac{1}{2})\phi] \end{pmatrix}. \quad (23)$$

The factor  $\sqrt{\rho}$  is introduced in the definition of the wave function  $U_m(\rho, z, t)$  [46] in order to simplify the integration over the variable  $\rho$  in the matrix elements of the Dirac and unit operators. The normalization condition of the wave function is given by

$$\langle \psi_m | \psi_m \rangle = \int_{-\infty}^{\infty} dz \int_0^{\infty} d\rho U_m^+(\rho, z, t) U_m(\rho, z, t) = 1. \quad (24)$$

Substituting Eq. (23) into the Dirac equation (1), we obtain

$$i \frac{\partial}{\partial t} U_m(\rho, z, t) = \hat{H}_C U_m(\rho, z, t), \quad (25)$$

where the Hermitian operator  $\hat{H}_C$  is the cylindrical part of the Dirac operator

$$\hat{H}_C = \begin{pmatrix} V & 0 & c \frac{\partial}{\partial z} & \hat{K} \\ 0 & V & -\hat{K}^+ & -c \frac{\partial}{\partial z} \\ -c \frac{\partial}{\partial z} & -\hat{K} & V - 2c^2 & 0 \\ -\hat{K}^+ & c \frac{\partial}{\partial z} & 0 & V - 2c^2 \end{pmatrix}, \quad (26)$$

$$\hat{K} = c \left( \frac{\partial}{\partial \rho} + \frac{m}{\rho} \right). \quad (27)$$

We solve the time-dependent Dirac equation (25), using the finite basis expansion in both  $\rho$  and  $z$  variables

$$U^k(\rho, z, t) = \sum_{\alpha, \mu} \sum_{\beta, \nu} C_{\alpha\mu, \beta\nu}^k(t) s_{\alpha}^{\mu}(\rho) s_{\beta}^{\nu}(z). \quad (28)$$

Here index  $k = 1, 2, 3, 4$  enumerates the  $U(\rho, z, t)$  components. The coefficients  $C(t)$  can be found solving the time-dependent matrix equation (4).

### E. Full 3D approach

In the 3D case we use the Cartesian coordinates  $(x, y, z)$  and the finite basis spline expansion of the wave function  $\psi(\mathbf{r}, t)$  in the form

$$\psi^k(x, y, z, t) = \sum_{\alpha, \mu} \sum_{\beta, \nu} \sum_{\gamma, \lambda} C_{\alpha\mu, \beta\nu, \gamma\lambda}^k(t) s_{\alpha}^{\mu}(x) s_{\beta}^{\nu}(y) s_{\gamma}^{\lambda}(z). \quad (29)$$

The index  $k = 1, 2, 3, 4$  enumerates the components of the Dirac bispinor, indices  $\mu, \nu, \lambda = 0, 1$  denote the type of the cubic Hermite splines, and indices  $\alpha, \beta, \gamma$  label the splines, centered at the different points. The total number of the basis functions is equal to  $N = 4 \cdot 2N_x \cdot 2N_y \cdot 2N_z$ , where  $N_x, N_y$  and  $N_z$  are the numbers of grid points in the  $x, y$ , and  $z$  directions, respectively.

In the 3D case we are faced with the huge sparse overlapping  $S$  and Hamiltonian  $H(t)$  matrices. It is possible to store only nonzero elements of these matrices in computer memory. Solving the time-dependent equation by the CN method (10) we have to calculate the inverse  $S^{-1}$  matrix. A fast algorithm based on factorization of the overlapping matrix into Kronecker's (direct) matrix production  $S = S_x \otimes S_y \otimes S_z$  and the inverse matrix calculation [47]  $S^{-1} = S_x^{-1} \otimes S_y^{-1} \otimes S_z^{-1}$  are used.

Eq. (10) is solved by the stabilized biconjugate gradient method [48]. The generalization of this method for the case of complex matrices is given in Ref. [49].

The coefficients  $C$  at the initial time point can be determined using the interpolation properties of the cubic Hermite splines (15)

$$C_{\alpha\mu, \beta\nu, \gamma\lambda}^k = \left( \frac{\partial}{\partial x} \right)^{\mu} \left( \frac{\partial}{\partial y} \right)^{\nu} \left( \frac{\partial}{\partial z} \right)^{\lambda} \psi_0^k(x, y, z) \Big|_{x_{\alpha}, y_{\beta}, z_{\gamma}}, \quad \mu, \nu, \lambda = 0, 1, \quad (30)$$

where  $\psi_0(x, y, z)$  is the ground state wave function of the H-like ion in the central-field approximation.

### F. Transition amplitudes. Contribution of the negative-energy Dirac continuum

We consider here, for simplicity, one-center transitions between the target states, assuming that the target is at rest. For the one-electron system the transition amplitude is defined by

$$T_{ji} = \langle \psi_j^{(0)}(t) | \psi_i(t) \rangle, \quad t \rightarrow \infty, \quad (31)$$

where  $\psi_j^{(0)}(\mathbf{r}, t) = e^{-i\varepsilon_j t} \phi_j(\mathbf{r})$  is a one-electron stationary wave function of the unperturbed target Hamiltonian ( $\hat{H}^{(0)} \phi_j = \varepsilon_j \phi_j$ ) and  $\psi_i(\mathbf{r}, t)$  is the wave function of the colliding system with the initial

condition:

$$\psi_i(\mathbf{r}, t) \rightarrow e^{-i\varepsilon_i t} \phi_i(\mathbf{r}), \quad t \rightarrow -\infty. \quad (32)$$

The corresponding probability is equal to  $P_{ji} = |T_{ji}|^2$ . In particular, the probability to find the electron after the collision in the ground  $1s$  state of the target is

$$P_{1s} = |\langle \psi_{1s}^{(0)}(t) | \psi_{1s}(t) \rangle|^2, \quad t \rightarrow \infty. \quad (33)$$

Formally, we can also define the total transition probability  $P^{(-)}$  to the negative-energy states

$$P^{(-)} = \sum_j^{\varepsilon_j \leq -2c^2} |\langle \psi_j^{(0)}(t) | \psi_{1s}(t) \rangle|^2, \quad t \rightarrow \infty. \quad (34)$$

To be closer to the real situation, we should consider the many-electron picture, where all the negative-energy continuum states are occupied by electrons according to the Pauli principle. Then, neglecting the electron-electron interaction, the one-electron wave functions  $\psi_{1s}^{(0)}(\mathbf{r}, t)$  and  $\psi_{1s}(\mathbf{r}, t)$  in Eq. (33) have to be replaced by the Slater determinants

$$\Psi_{1s}^{(0)}(\mathbf{r}_1, \dots, \mathbf{r}_{N_e}, t) = \frac{1}{\sqrt{N_e!}} \det\{\psi_k^{(0)}(\mathbf{r}_l, t)\}, \quad \Psi_{1s}(\mathbf{r}_1, \dots, \mathbf{r}_{N_e}, t) = \frac{1}{\sqrt{N_e!}} \det\{\psi_k(\mathbf{r}_l, t)\}, \quad (35)$$

where  $N_e$  is the number of electrons, that includes the one  $1s$  and all negative-energy continuum electrons. Then, the corrected probability  $\bar{P}_{1s}$  to find the system after the collision in the ground  $1s$  state is given by

$$\bar{P}_{1s} = |\langle \Psi_{1s}^{(0)}(t) | \Psi_{1s}(t) \rangle|^2 = |\det\{\langle \psi_k^{(0)}(t) | \psi_l(t) \rangle\}|^2, \quad (36)$$

where  $k$  and  $l$  run over the one  $1s$  and all negative-energy continuum states. In deriving Eq. (36) we have used the fact that the scalar product of two Slater determinants is equal to the determinant of the scalar product of the one-electron wave functions [50].

The calculation of the corrected probability  $\bar{P}_{1s}$  is much more time consuming than the calculation of  $P_{1s}$ . In the present paper we performed this calculation in the 1D case only.

We note that the same result, which is given by Eq. (36), can be obtained using the second quantization formalism [51].

### III. RESULTS OF THE CALCULATIONS AND DISCUSSION

In this section we present the results of the calculations within the monopole (1D) and axially-symmetric (2D) approximations, and the full 3D approach. We consider the straight-line collision of the

H-like uranium (target,  $A$ ) being initially in the ground state with the bare uranium nucleus (projectile,  $B$ ) at the 6 MeV/u energy and the impact parameter  $b$  (see Fig. 1). We choose the coordinate system with the origin at the center of the fixed target and the  $z$ -axis parallel to the straight-line trajectory of the projectile. Unless stated otherwise, the model of the nuclear charge distribution employed is a uniformly charged sphere of radius  $R_n = \sqrt{5/3}R_{\text{RMS}}$ , where  $R_{\text{RMS}}$  is the root-mean-square nuclear radius. Then the Coulomb potential of the nucleus is given by

$$V_{\text{nucl}}(r) = \begin{cases} -\frac{Z}{r} & r \geq R_n \\ -\frac{Z}{2R_n} \left( 3 - \frac{r^2}{R_n^2} \right) & r < R_n \end{cases}. \quad (37)$$

According to Ref. [52], we use  $R_{\text{RMS}} = 5.8569(33)$  fm for the uranium nuclear radius.

#### A. Monopole approximation (1D)

In the monopole approximation we use the basis set of 384 splines (96 grid points) that is sufficient to obtain the results with a high accuracy. This can be seen from Table I, where we compare our data for the energy of the  $1s$  state of H-like ions, calculated for the point-charge nucleus in the finite basis approximation, with the exact analytical values.

The semi-logarithmic grid  $\zeta_\alpha = \eta r_\alpha + \xi \ln(r_\alpha)$ , proposed by Brattsev [53] and widely used in nonrelativistic [54] and relativistic [55] atomic calculations, is employed to generate the set of points  $r_\alpha$  (points  $\zeta_\alpha$  are taken with a constant step).

TABLE I: The  $1s$  state energy of H-like ions (in a.u.) for the point-charge nucleus.

Z	Finite basis	Exact values
92	-4861.1979	-4861.1979
100	-5939.1952	-5939.1952
130	-12838.926	-12838.920

In the monopole approximation we can not calculate the charge transfer probabilities. However, we can evaluate the  $1s$  state target population probability  $P_{1s}(b)$  (probability to stay in the  $1s$  target state after the collision) and the transition probability to the negative-energy continuum states  $P^{(-)}(b)$

as functions of the impact parameter  $b$ . The collision was considered in a spherical box, with the target placed at the box center. The radius of the box was taken to be  $19/Z$  a.u.  $\simeq 10924$  fm. This value should be compared with the mean radius of the  $1s$  orbital of H-like uranium equal to  $\langle r \rangle \simeq 0.0135$  a.u.  $\simeq 713$  fm.

TABLE II: The average energy  $E_{\min}(b)$  at the minimal internuclear distance ( $R = b$ ), as a function of the impact parameter  $b$  (in fm). The calculations are performed for the point-like and uniformly charged sphere nuclear models ( $R_{\text{RMS}} = 5.8569$  fm). The monopole (1D) approximation is used.

$E_{\min}/mc^2 + 1$		
$b$	Point-charge nucleus	Sphere nuclear model
15	-1.353	-1.224
20	-1.124	-1.046
25	-0.967	-0.913
30	-0.849	-0.810
40	-0.680	-0.656
50	-0.561	-0.545

In Table II we present the results of our calculations for the minimal energy  $E_{\min}(b)$ , as a function of the impact parameter  $b$ . The minimal energy  $E_{\min}(b)$  was calculated as the expectation value of the time-dependent Hamiltonian  $\hat{H}(t)$  (see Eq. (21)) at the shortest internuclear distance  $R(0) = b$ , which corresponds to  $t = 0$ . As one can see from Table II, the average energy  $E_{\min}(t, b)$  dives into the negative-energy continuum at the impact parameter slightly bigger than  $b = 20$  fm. It should be noticed that the stationary  $1s$  state of the quasi-molecule calculated within the 1D model for the point-charge nucleus dives into the negative-energy continuum at the critical internuclear distance  $R_{\text{cr}} = 25.5$  fm [28].

In Table III we present the results of our calculations for the  $1s$  population probability  $P_{1s}(b)$  and the negative-energy continuum population probability  $P^{(-)}(b)$  as functions of the impact parameter  $b$ . The  $1s$  population probability  $P_{1s}(b)$  was calculated in the one-electron picture.

We also calculated the corrected  $1s$  population probability  $\bar{P}_{1s}(b)$  within the many-electron picture, described in Sec II F. The calculations have been performed for the point-like and uniformly charged

TABLE III: The population probability of the  $1s$  target state  $P_{1s}(b)$  and the negative-energy continuum population probability  $P^{(-)}(b)$  at the infinite time limit ( $t \rightarrow \infty$ ) as functions of the impact parameter  $b$  (in fm). The monopole (1D) approximation is used.

	Point-charge nucleus		Sphere nuclear model	
$b$	$P_{1s}$	$P^{(-)}$	$P_{1s}$	$P^{(-)}$
15	0.549435	$4.70 \times 10^{-3}$	0.610272	$3.43 \times 10^{-3}$
20	0.669281	$2.59 \times 10^{-3}$	0.706189	$2.00 \times 10^{-3}$
30	0.811566	$0.87 \times 10^{-3}$	0.826959	$0.72 \times 10^{-3}$
40	0.886131	$0.32 \times 10^{-3}$	0.893379	$0.27 \times 10^{-3}$
50	0.928079	$0.12 \times 10^{-3}$	0.931794	$0.11 \times 10^{-3}$

TABLE IV: The population probability of the  $1s$  target state calculated within the one-electron ( $P_{1s}(b)$ ) and many-electron ( $\overline{P}_{1s}(b)$ ) pictures as a function of the impact parameter  $b$  (in fm). The calculations are performed for the point-like and uniformly charged sphere nuclear models ( $R_{\text{RMS}} = 5.8569$  fm). The monopole (1D) approximation is used.

	Point-charge nucleus		Sphere nuclear model	
$b$	$\overline{P}_{1s}$	$\overline{P}_{1s} - P_{1s}$	$\overline{P}_{1s}$	$\overline{P}_{1s} - P_{1s}$
15	0.550244	$8.09 \times 10^{-4}$	0.610755	$4.84 \times 10^{-4}$
20	0.669606	$3.25 \times 10^{-4}$	0.706402	$2.14 \times 10^{-4}$
30	0.811627	$0.61 \times 10^{-4}$	0.827004	$0.45 \times 10^{-4}$
40	0.886144	$0.13 \times 10^{-4}$	0.893389	$0.11 \times 10^{-4}$
50	0.909947	$0.03 \times 10^{-4}$	0.931796	$0.03 \times 10^{-4}$

sphere nuclear models. The obtained values are presented in Table IV. The comparison of the  $\overline{P}_{1s}(b)$  data with the values obtained in the one-electron picture shows that the role of the negative-energy continuum is rather small, and a larger effect comes from the nuclear charge distribution.

The high probability of staying in the initial state of the target can be explained by the fact that the velocity of the incident particle  $v_p$  is much smaller than the velocity of electron motion  $v_e$  in the nuclear

field,  $v_p/v_e \sim 0.16$ .

### B. Axial-symmetry approximation (2D)

In the axial-symmetry approximation the calculations were performed using 200 splines (100 grid points) along the  $z$  axis and 52 splines (26 grid points) for the variable  $\rho$  on the uniform grid. Thus, the total number of the basis functions was equal to  $4 \times 200 \times 52 = 41600$ . The cylindrical box  $20000 \times 5000 \text{ fm}^2$  was used, and the target position was shifted by 5000 fm from the box center along the  $z$  axis in the direction of the initial projectile position. This was done to minimize the influence of the box borders on the time-dependent wave function after the collision. The number of time steps, which was used to solve the time-dependent equation, was equal to 15000. The point-charge nuclear model was used for both colliding nuclei. The initial  $1s$  wave function, localized at the target ion, was calculated as an eigenfunction of the Hamiltonian matrix in the same basis set. The obtained energy value,  $-4849 \text{ a.u.}$ , is close to the exact one, which is equal to  $-4861 \text{ a.u.}$

The charge-transfer probability  $P_{\text{ct}}(b)$  was calculated by dividing the entire space into two equal parts and integrating the final electron density over the part with the projectile. The values of  $P_{\text{ct}}(b)$  obtained in the 2D approximation and in the full 3D approach (the corresponding details are given in the next subsection), and also the related data from Ref. [28] are presented in Fig. 3. The evaluation was done within the one-electron picture. One can observe a rather good agreement between the 2D and full 3D results for the charge-transfer probability.

### C. Full 3D approach

In the 3D case the charge-transfer probability was calculated using  $40 \times 40 \times 80$  splines for each component of the four component relativistic wave function on the 3D  $(x, y, z)$  uniform space grid. The total size of the finite basis set was equal to 512000. The point-charge nuclear model was used for both colliding nuclei. The  $\text{U}^{91+}(1s)$  initial state energy calculated with this basis is equal to  $-4711 \text{ a.u.}$ , that fairly agrees with the exact energy value.

The rectangular box  $6900 \times 6900 \times 13800 \text{ fm}^3$  was used in the 3D calculations and, as in the 2D case, the target position was shifted from the box center along the  $z$  axis in the direction of the initial projectile position by the value equal to a quarter of the box length. The time-dependent equation was solved using the CN method with 1024 time steps. Again, the one-electron picture was used.

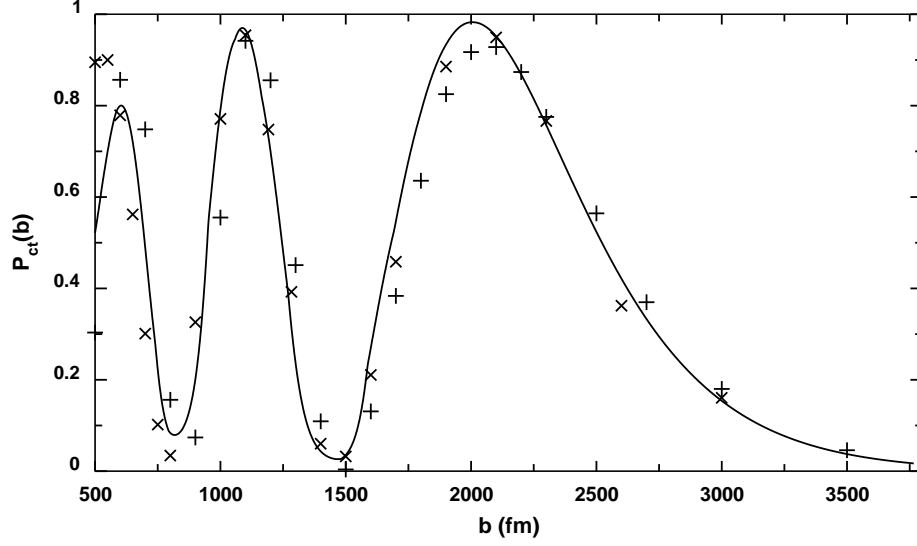


FIG. 3: The charge-transfer probability  $P_{ct}(b)$  as a function of the impact parameter  $b$ . The signs “+” and “x” indicate the 2D and 3D results, respectively. The solid line shows the results from Ref. [28].

The values of the charge-transfer probability  $P_{ct}(b)$  obtained with the 3D approach are shown in Fig. 3. The results are in good agreement with the data obtained in Ref. [28].

#### IV. CONCLUSION

In this paper we presented a new method for the relativistic calculations of one-electron two-center quasi-molecular systems in both stationary and time-dependent regimes using the finite basis set of cubic Hermite splines. The calculations were performed for the low-energy  $U^{91+}(1s)-U^{92+}$  collision at the projectile energy 6 MeV/u within the 1D, 2D and 3D approaches.

In the 1D approximation we examined the influence of the negative-energy Dirac continuum on the  $1s$  population probability. It was found that this influence is rather small. It should also be noted that the probability to find the electron in the  $1s$  state of the target after the collision, calculated in the monopole approximation, is quite large. This shows the adiabatic nature of the collision process.

The charge-transfer probabilities were evaluated in the 2D approximation and in the full 3D approach using the one-electron picture. The results of the calculations are in a good agreement with each other, that also indicates the adiabatic nature of the collision process. The obtained results agree also with our previous calculations performed by the Dirac-Sturm method [28].



## **Acknowledgments**

We thank S. Hagmann and C. Kozhuharov for many helpful discussions. This work was supported by RFBR (Grants No. 13-02-00630 and No. 11-02-00943-a), by the Ministry of Education and Science of the Russian Federation (Grant No. 8420), by GSI, by DAAD, and by the grant of the President of the Russian Federation (Grant No. MK-2106.2012.2). The work of I.A.M. was also supported by the Dynasty foundation. I.A.M., A.I.B., and Y.S.K. acknowledge financial support by the FAIR–Russia Research Center.

## Appendix: Crank-Nicolson method for the finite basis time-dependent equation in the non-orthogonal basis

Consider the time-dependent Dirac equation in the finite basis set

$$i S \frac{d\mathbf{C}^i(t)}{dt} = H(t) \mathbf{C}^i(t), \quad \psi_i(\mathbf{r}, t) = \sum_k C_k^i(t) \varphi_k(\mathbf{r}). \quad (\text{A1})$$

Here the index  $i$  enumerates different solutions of the time-dependent equation. In the Crank-Nicolson approximation the coefficients  $\mathbf{C}^i(t + \Delta t)$  can be determined from the coefficients  $\mathbf{C}^i(t)$  by solving the system of linear equations

$$\left[ S + \frac{i\Delta t}{2} H \right] \mathbf{C}^i(t + \Delta t) = \left[ S - \frac{i\Delta t}{2} H \right] \mathbf{C}^i(t). \quad (\text{A2})$$

Let us rewrite this equation in the following way

$$S^{1/2} \left[ 1 + \frac{i\Delta t}{2} H^{(L)} \right] S^{1/2} \mathbf{C}^i(t + \Delta t) = S^{1/2} \left[ 1 - \frac{i\Delta t}{2} H^{(L)} \right] S^{1/2} \mathbf{C}^i(t), \quad (\text{A3})$$

where  $H^{(L)}$  is the Hamiltonian matrix in the Löwdin representation [56]

$$H^{(L)} \equiv S^{-1/2} H S^{-1/2}.$$

Eq. (A3) is conveniently written in the form

$$\mathbf{C}^i(t + \Delta t) = U_{\text{CN}} \mathbf{C}^i(t), \quad (\text{A4})$$

where the matrix  $U_{\text{CN}}$  is given by

$$U_{\text{CN}} \equiv S^{-1/2} (V^{-1})^+ V S^{1/2}, \quad (\text{A5})$$

with

$$V \equiv \left[ 1 - \frac{i\Delta t}{2} H^{(L)} \right]. \quad (\text{A6})$$

The matrices  $V$  and  $V^+$  commute, since  $H^{(L)}$  is an Hermitian matrix. We obtain

$$U_{\text{CN}} S U_{\text{CN}}^+ = \left( S^{1/2} V^{-1+} V S^{-1/2} \right) S \left( S^{-1/2} V^+ V^{-1} S^{1/2} \right) = S$$

and

$$\mathbf{C}^{i+}(t + \Delta t) S \mathbf{C}^j(t + \Delta t) = \mathbf{C}^{i+}(t) U_{\text{CN}}^+ S U_{\text{CN}} \mathbf{C}^j(t) = \mathbf{C}^{i+}(t) S \mathbf{C}^j(t). \quad (\text{A7})$$

Thus, the Crank-Nicolson approximation preserves the norm of the wave function

$$\langle \psi_i(t + \Delta t) | \psi_j(t + \Delta t) \rangle = \mathbf{C}^{i+}(t + \Delta t) S \mathbf{C}^j(t + \Delta t) = \langle \psi_i(t) | \psi_j(t) \rangle. \quad (\text{A8})$$

- 
- [1] J. Eichler and W. E. Meyerhof, *Relativistic Atomic Collisions*, (Academic Press, New York, 1995).
- [2] V. M. Shabaev, Phys. Rep. **356**, 119 (2002).
- [3] J. Eichler and Th. Stöhlker, Phys. Rep. **439**, 1 (2007).
- [4] I. Yu. Tolstikhina and V. P. Shevelko, Physics-Uspekhi **56**, 213 (2013).
- [5] W. Greiner, B. Müller, J. Rafelski, *Quantum Electrodynamics of Strong Fields*, (Springer-Verlag, Berlin, 1985).
- [6] U. Becker, N. Grün, W. Scheid, and G. Soff, Phys. Rev. Lett. **56**, 2016 (1986).
- [7] M. R. Strayer, C. Bottcher, V. E. Oberacker, and A. S. Umar, Phys. Rev. A **41**, 1399 (1990).
- [8] J. Thiel, A. Bunker, K. Momberger, N. Grün, and W. Scheid, Phys. Rev. A **46**, 2607, (1992).
- [9] J. C. Wells, V. E. Oberacker, A. S. Umar, C. Bottcher, M. R. Strayer, J.-S. Wu, and G. Plunien, Phys. Rev. A **45**, 6296 (1992).
- [10] J. C. Wells, V. E. Oberacker, M. R. Strayer, and A. S. Umar, Phys. Rev. A **53**, 1498 (1996).
- [11] M. S. Pindzola, Phys. Rev. A **62**, 032707 (2000).
- [12] O. Busic, N. Grün and W. Scheid, Phys. Rev. A **70**, 062707 (2004).
- [13] K. Momberger, A. Belkacem, and A. H. Sørensen, Phys. Rev. A **53**, 1605 (1996).
- [14] D. C. Ionescu and A. Belkacem, Phys. Scr. **80**, 128 (1999).
- [15] J. Eichler, Phys. Rep. **193**, 165 (1990).
- [16] K. Rumrich, G. Soff, W. Greiner, Phys. Rev. A **47**, 215 (1993).
- [17] K. Momberger, N. Grün, and W. Scheid, J. Phys. B **26**, 1851 (1993).
- [18] M. Gail, N. Grün and W. Scheid, J. Phys. B **36**, 1397 (2003).
- [19] P. Küprick, H. J. Lüdde, W.-D. Sepp, B. Fricke, Z. Phys. D **25**, 17 (1992).
- [20] P. Küprick, W.-D. Sepp, B. Fricke, Phys. Rev. A **51**, 3693 (1995).
- [21] B. Müller, J. Rafelski, and W. Greiner, Z. Phys. **257**, 183 (1972).
- [22] G. Soff, J. Reinhardt, and W. Betz, Phys. Scr. **17**, 417 (1978).
- [23] T. H. J. de Reus, J. Reinhardt, B. Müller, W. Greiner, G. Soff, and U. Müller, J. Phys. B **17**, 615 (1984).
- [24] E. Ackad and M. Horbatsch, Phys. Rev. A **78**, 062711 (2008).
- [25] U. Müller-Nehler and G. Soff, Phys. Rep. **246**, 101 (1994).
- [26] A. Marsman and M. Horbatsch, Phys. Rev. A **84**, 032517 (2011).

- [27] S. R. McConnell, A. N. Artemyev, M. Mai, and A. Surzhykov, Phys. Rev. A **86**, 052705 (2012).
- [28] I. I. Tupitsyn, Y. S. Kozhedub, V. M. Shabaev, G. B. Deyneka, S. Hagmann, C. Kozhuharov, G. Plunien, and Th. Stöhlker, Phys. Rev. A **82**, 042701 (2010).
- [29] I. I. Tupitsyn, Y. S. Kozhedub, V. M. Shabaev, A. I. Bondarev, G. B. Deyneka, I. A. Maltsev, S. Hagmann, G. Plunien, and Th. Stöhlker, Phys. Rev. A **85**, 032712 (2012).
- [30] Y. S. Kozhedub, I. I. Tupitsyn, V. M. Shabaev, S. Hagmann, G. Plunien and Th. Stöhlker, Phys. Scr. **156**, 014053 (2013).
- [31] A. I. Bondarev, Y. S. Kozhedub, I. I. Tupitsyn, V. M. Shabaev and G. Plunien, Phys. Scr. **156**, 014054 (2013).
- [32] I. A. Maltsev, G. B. Deyneka, I. I. Tupitsyn, V. M. Shabaev, Y. S. Kozhedub, G. Plunien and Th. Stöhlker, Phys. Scr. **156**, 014056 (2013).
- [33] G. B. Deineka, Int. J. Quant. Chem. **100**, **4**, 677 (2004).
- [34] G. B. Deineka, Int. J. Quant. Chem. **106**, 2262 (2006).
- [35] C. de Boor, *A Practical Guide to Splines*, Applied Mathematical Sciences, Rev.ed., Springer, NY **27**, (2001).
- [36] W. R. Johnson, S. A. Blundell and J. Sapirstein, Phys. Rev. A **37**, 307 (1988).
- [37] V. M. Shabaev, I. I. Tupitsyn, V. A. Yerokhin, G. Plunien, and G. Soff, Phys. Rev. Lett. **93**, 130405 (2004).
- [38] A. N. Artemyev, E. V. Ludena, V. V. Karasiev and A. J. Hernández, J. Comput. Chem. **25**, 368 (2004).
- [39] A. N. Artemyev, A. Surzhykov, P. Indelicato, G. Plunien and Th Stöhlker, J. Phys. B **43**, 235207 (2010).
- [40] J. C. Morrison, C. Baunach, L. Larson, B. Bialecki and G. Fairweather, J. Phys. B **29** 2375 (1996).
- [41] J. C. Morrison, T. Wolf, B. Bialecki, G. Fairweather, L. Larson, Mol. Phys. **98** 1175 (2000).
- [42] G. B. Deineka, Optics and Spectroscopy **81**, 159 (1996).
- [43] T. Ozaki, M. Toyoda, Comp. Phys. Comm. **182**, 1245 (2011).
- [44] J. Crank, P. Nicolson, Proc. Cambridge Philos. Soc. **43**, 50 (1947).
- [45] R. S. Varga, *Matrix Iterative Analysis*, Springer Series in Computational Mathematics, **27**, Springer-Verlag, Berlin-Heidelberg (2000).
- [46] P. Schlüter, K-H. Wietschorke, W. Greiner, J. Phys. A **16**, 1999 (1983).
- [47] P. Lancaster, M. Tismenetsky, *The Theory of Matrices*, (2-nd Ed., Academic Press, NY, 1985).
- [48] Y. Saad, *Iterative Methods for Sparse Linear Systems*, (2-nd Ed., SIAM, Philadelphia, 2003).
- [49] P. Joly, *Numerical Algorithms*, **4**, 379 (1993).
- [50] R. McWeeny, *Methods of Molecular Quantum Mechanics*, (2-nd Ed., Academic Press, 2001).

- [51] E. S. Fradkin, D. M. Gitman, and S. M. Shvartsman, *Quantum Electrodynamics with Unstable Vacuum*, (Springer-Verlag, Berlin, 1991).
- [52] Y. S. Kozhedub, O. V. Andreev, V. M. Shabaev, I. I. Tupitsyn, C. Brandau, C. Kozhuharov, G. Plunien, and T. Stöhlker, Phys. Rev. A **77**, 032501 (2008).
- [53] V. F. Brattsev, *Tables of Wave Functions* (in Russian), Nauka, Moscow (1966).
- [54] L. V. Chernysheva, N. A. Cherepkov and V. Radojević, Comput. Phys. Commun. **11** 57 (1976).
- [55] V. F. Brattsev, G. B. Deineka and I. I. Tupitsyn, Izv. Akad. Nauk SSSR (in Russian) **41**, 2655 (1977); [Bull. Acad. Sci. USSR Phys Ser. **41**, 173 (1977)].
- [56] P. O. Löwdin, J. Chem. Phys **18**, 365 (1950).